

LETTERS

PACS numbers: 42.25.Gy; 32.10.Bi; 78.20.Ci
DOI: 10.1070/QE2010v040n09ABEH014399

Near- to mid-IR refractive index of ^{28}Si, ^{29}Si and ^{30}Si monoisotopic single crystals

V. G. Plotnichenko, V.O. Nazaryants, E.B. Kryukova, V.V. Koltashev, V.O. Sokolov, A.V. Gusev, V.A. Gavva, M.F. Churbanov, E.M. Dianov

***Abstract*. We have prepared ^{28}Si, ^{29}Si and ^{30}Si single crystals with enrichments above 99.9 at % and a silicon single crystal of natural isotopic composition. The oxygen and carbon concentrations in all the crystals are within 5×10^{15} cm^{-3}, and the content of metal impurities is 0.01 – 0.1 ppma. The refractive index of the crystals has been determined in the range 1.05 – 25.5 μm using interference refractometry, and its dispersion and material dispersion have been determined.**

Keywords: *silicon; ^{28}Si, ^{29}Si and ^{30}Si single crystals; refractive index*.

Crystalline silicon is the basic material of microelectronics and solar cells. In addition, it is an attractive optical material with a high transmission in the near- to mid-IR spectral region. Recent years have seen rapid growth in silicon photonics, which is expected to find application in next-generation optical fibre communication and information transfer systems. Monoisotopic silicon is considered the basic component of quantum computers [1].

Polycrystalline silicon was prepared earlier by thermal decomposition of silane enriched in one of the silicon isotopes. The preparation of high-purity isotopically enriched silane was described by Devyatykh et al. [2] and Churbanov et al. [3]. The process was run on a graphite substrate at 800 °C. The resultant silicon was separated from the substrate and purified by ten molten zone passes. Single crystals were grown in the [100] direction by float zoning in a high-purity argon atmosphere. The same procedure was used to prepare a single crystal of natural isotopic composition, ^{nat}Si: 92.23% ^{28}Si, 4.68% ^{29}Si, 3.09% ^{30}Si [4].

The isotopic composition of the crystals was determined by mass spectrometry [5] with an accuracy of 0.01 at % or better. The results are presented in Table 1. Comparison with data reported by Itoh et al. [6] and Ager et al. [7] indicates that our crystals are more isotopically enriched and offer higher chemical purity and resistivity.

Table 1. Isotopic composition of the Si single crystals (mass spectrometry data)

Crystal	Atomic percent		
	^{28}Si	^{29}Si	^{30}Si
^{28}Si	99.9934	0.00637	0.00023
^{29}Si	0.026	99.919	0.055
^{30}Si	0.005	0.021	99.974

The structural perfection of the crystals was evaluated using X-ray diffraction and selective etching. No orientation disorder, low-angle boundaries or twin regions were detected in the crystals. The width of their rocking curves was 11″ – 12″. The room-temperature resistivity of the crystals ranged from 100 to 200 Ω cm.

According to mass spectrometric measurements, the contents of 72 impurities were below the detection limit of mass spectrometry (less than 0.01 – 0.1 ppma). The oxygen and carbon concentrations were within 5×10^{15} cm^{-3} as determined by IR spectroscopy in conformity with the ASTM standards F-1188 and F-1391 [8].

Figure 1 shows the room-temperature Raman spectra of the four crystals. The spectra were measured in a backscattering geometry on a T64000 triple spectrograph. Excitation was provided by the 514.5-nm argon laser line. The detector used was a liquid nitrogen cooled CCD matrix, which enabled the spectra to be collected in 0.7-cm^{-1} steps. The observed Raman band (data points in Fig. 1), due to first-order scattering by phonons of Γ_{15} symmetry, is well fitted by a Lorentzian of width 3.3 – 3.4 cm^{-1} for ^{28}Si, ^{29}Si and ^{30}Si and 3.7 cm^{-1} for ^{nat}Si (solid lines), which points to high structural perfection of the monoisotopic single crystals.

Figure 2 plots the peak position of the Raman band against atomic mass for the four crystals. The solid line represents the best fit for the phonon frequency vs. atomic mass data: $\Omega = 2758.70M^{-1/2}$.

From the crystals, we prepared plane-parallel plates of three thicknesses (0.7 to 1.3 mm) for measuring interference

V. G. Plotnichenko, V.V. Koltashev, V.O. Sokolov, E.M. Dianov Fiber Optics Research Center, Russian Academy of Sciences, ul. Vavilova 38, 119333 Moscow, Russia; e-mail: victor@fo.gpi.ru, dianov@fo.gpi.ru, sokolov@fo.gpi.ru;
V.O. Nazaryants Tarusa Branch, A.M. Prokhorov General Physics Institute, Russian Academy of Sciences, ul. Engel'sa 6, 249100 Tarusa, Kaluga region, Russia; e-mail: nvo@fo.gpi.ru;
E.B. Kryukova V.I. Vernadsky Institute of Geochemistry and Analytical Chemistry, Russian Academy of Sciences, ul. Kosygina 19, 119991 Moscow, Russia; e-mail: elena@fo.gpi.ru;
A.V. Gusev, V.A. Gavva, M.F. Churbanov Institute of Chemistry of High-Purity Substances, Russian Academy of Sciences, ul. Tropinina 49, 603950 Nizhnii Novgorod, Russia; e-mail: gusev@ihps.nnov.ru

Received 14 July 2010
Kvantovaya Elektronika **40** (9) 753 – 755 (2010)
Translated by O.M. Tsarev

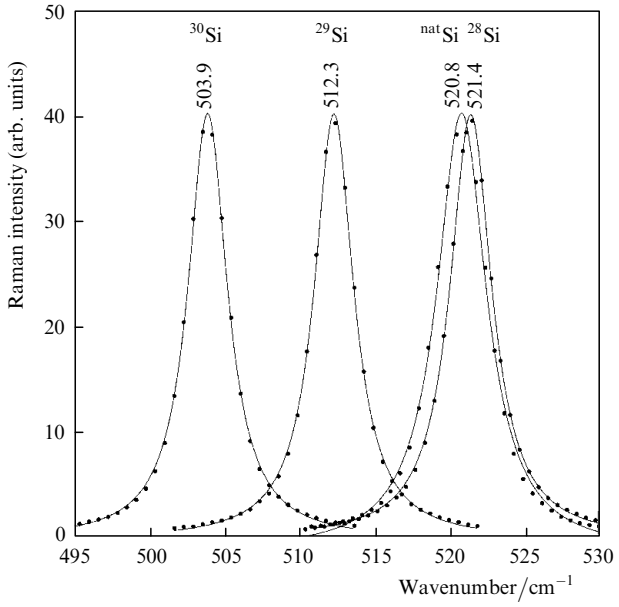

Figure 1. Fundamental Raman band of the ^{28}Si, ^{29}Si, ^{30}Si and ^{nat}Si (natural isotopic composition) single crystals.

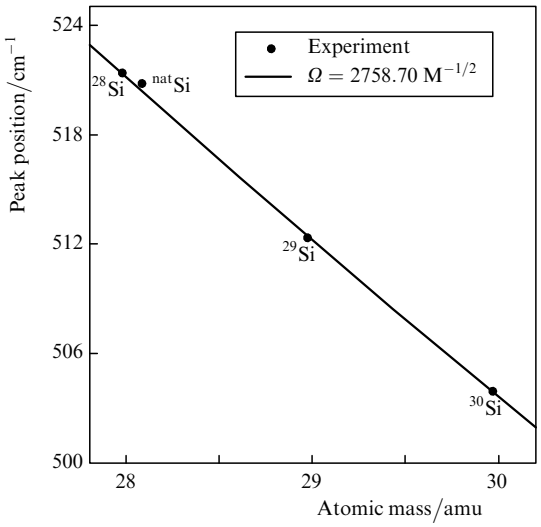

Figure 2. Peak position of the Raman band, Ω, as a function of atomic mass.

transmission spectra. The measurements were made on a Bruker IFS-113v Fourier transform vacuum spectrometer in the range 9500–390 cm^{-1} (1.05–25.5 μm) with a resolution of 0.1 cm^{-1}. Each interference maximum was obtained as at least ten data points. The sample temperature was maintained at 22 °C with a stability of 0.1 °C. The spectra were used to determine the refractive index n of the crystals as described in [9, 10]. The data set thus obtained (more than 70000 n values) was fitted with a Cauchy polynomial of the eighth degree [11],

$$n(\lambda_m) = A_8\lambda_m^8 + A_6\lambda_m^6 + A_4\lambda_m^4 + A_2\lambda_m^2 + C + B_2/\lambda_m^2 + B_4/\lambda_m^4 + B_6/\lambda_m^6 + B_8/\lambda_m^8,$$

which ensured an rms deviation in n within 3.5×10^{-5} over the entire measured range and a maximum deviation less

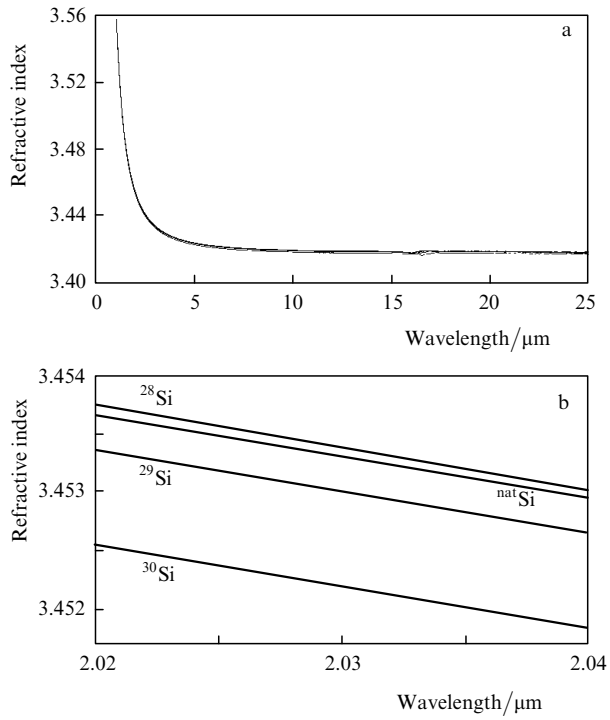

Figure 3. Spectral dependences of the refractive index for the ^{28}Si, ^{29}Si, ^{30}Si and ^{nat}Si (natural isotopic composition) single crystals (a) over the entire measured range and (b) in the range 2.02–2.04 μm.

than 2×10^{-4}. Figure 3 shows the spectral dependences of n for the isotopically enriched and natural Si crystals. Table 2 lists the refractive indices of the silicon crystals at 1.5, 2 and 5 μm.

Table 2. Refractive index of the silicon single crystals at 1.5, 2 and 5 μm.

Crystal	Wavelength/μm		
	1.5	2	5
^{28}Si	3.48399	3.45446	3.42385
^{nat}Si	3.48392	3.45432	3.42374
^{29}Si	3.48358	3.45411	3.42344
^{30}Si	3.48268	3.45328	3.42266

It is seen in Fig. 3 that, with increasing atomic mass, the spectral dependence of the refractive index far away from electron and phonon transitions shifts downwards. This behaviour of the dispersion curve can be understood in terms of a lattice of coupled dipoles [12, 13]. In this classic model, the following relation holds for a cubic lattice with no absorption and no spatial dispersion:

$$n^2(\omega) = 1 - \frac{\alpha E_g(M_i)}{\omega^2 - E_g^2(M_i)} - \frac{\tilde{\beta}\Omega_i}{\omega^2 - \Omega_i^2},$$

where E_g is the band gap; M_i is the atomic mass of ^{i}Si; Ω_i is the phonon frequency; and α and $\tilde{\beta}$ are the model parameters representing two types of oscillators, corresponding to the fundamental absorption edges for electrons and phonons, respectively.

The intrinsic edge energies of an isotopically pure crystal can be expressed as [14–16]

$$E_g(T, M_i) = E_B - \alpha_B \left(\frac{M_{nat}}{M_i} \right)^{1/2} (1 + 2n_B),$$

$$\Omega_i = \Omega \left(\frac{M_{nat}}{M_i} \right)^{1/2},$$

where M_{nat} is the average atomic mass of natural Si and $n_B = (\exp \Omega_i/T - 1)^{-1}$ is the Bose distribution for phonons. According to Lastras-Martinez et al. [15] $E_B \approx 28713.3$ cm^{-1} and $\alpha_B \approx 967.9$ 967.9 cm^{-1}.

The α and $\tilde{\beta}$ parameters also depend on atomic mass. Moreover, both parameters vary with lattice constant as α_0^{-3}. Note that a_0 depends on atomic mass (see e.g. [17]), but this dependence is negligible in the test model under consideration. The vibrational parameter $\tilde{\beta}$ of silicon describes the IR absorption due to two-phonon transitions and, hence, is related to the atomic mass by

$$\tilde{\beta} = \frac{\beta}{M_i^2},$$

where $\beta = \text{const}$ [18]. Therefore, with increasing Si atomic mass, the electronic absorption edge shifts to shorter wavelengths, and the phonon absorption edge shifts to longer wavelengths. As a result, the dispersion curve of the refractive index in the transmission window should shift downwards without marked changes in shape, as observed in our experiments.

Thus, we have prepared and characterised high-purity ^{28}Si, ^{29}Si, ^{30}Si and ^{nat}Si single crystals. The refractive index of the crystals has been measured in a wide spectral range (1.05 – 25.5 μm).

The results demonstrate that the monoisotopic silicon crystals differ markedly in refractive index. This might be used to fabricate multilayer waveguiding structures from different silicon isotopes for integrated and fibre optics in the range from 1.05 to 25.5 μm.

Acknowledgements. We are grateful to I.D. Kovalev and A.M. Potapov for determining the isotopic and chemical compositions of the isotopically enriched silicon single crystals.

This work was supported by the Russian Foundation for Basic Research (Grant Nos 08-02-00964-a and 09-03-9741-R_povolzh'e_a), the RF President's Grants Council for Support to the Leading Scientific Schools of Russia (Grant No. NSh-4701.2008.3) and the Presidium of the Russian Academy of Sciences (basic research programmes Novel Optical Materials and Principles of Basic Research in Nanotechnologies and Nanomaterials).

References

1. Greenland P.T., Lynch S.A., van der Meer A.F.G., Murdin B.N., Pidgeon C.R., Redlich B., Vinh N.Q., Aeppli G. *Nature*, **465**, 1057 (2010).
2. Devyatykh G.G., Bulanov A.D., Gusev A.V., Kovalev I.D., Krylov V.A., Potapov A.M., Sennikov P.G., Adamchik S.A., Gavva V.A., Kotkov A.P., Churbanov M.F., Dianov E.M., Kaliteevskii A.K., Godisov O.N., Pohl H.J., Becker P., Riemann H., Abrosimov N.V. *Dokl. Akad. Nauk*, **391**, 638 (2003).
3. Churbanov M.F., Bulanov A.D., Kotkov A.P., Potapov A.M., Troshin O.Yu., Loshkov A.Yu., Grishnova N.D., Adamchik S.A. *Dokl. Akad. Nauk*, **432**, 60 (2010).
4. Rosman J.R., Taylor P.D. *Pure Appl. Chem.*, **70**, 217 (1998).
5. Kovalev I.D., Potapov A.M., Bulanov A.D. *Mass-Spektrom.*, **1**, 37 (2004).
6. Itoh K.M., Kato J., Uemura M., Kaliteevskii A.K., Godisov O.N., Devyatych G.G., Bulanov A.D., Gusev A.V., Kovalev I.D., Sennikov P.G., Pohl H.J., Abrosimov N.V., Riemann H. *Jpn. J. Appl. Phys.*, **42**, 6248 (2003).
7. Ager III J.W., Beeman J.W., Hansen W.L., Haller E.E., Sharp I.D., Liao C., Yang A., Thewalt M.W.L., Riemann H. *J. Electrochem. Soc.*, **152**, G448 (2005).
8. *Annual Book of ASTM Standards, Vol. 10.05 Electronics (II)*, 1996.
9. Plotnichenko V.G., Nazaryants V.O., Kryukova E.B., Pyrkov Yu.N., Dianov E.M., Galagan B.I., Sverchkov S.E. *Neorg. Mater.*, **45**, 366 (2009).
10. Plotnichenko V.G., Nazaryants V.O., Kryukova E.B., Dianov E.M. *J. Phys. D: Appl.Phys.*, **43**, 105402 (2010).
11. Smith D Y, Inokuti M, Karstens W. *J. Phys.: Condens. Matter,* **13**, 3883 (2001).
12. Fano U. *Phys. Rev.*, **118**, 451 (1960).
13. Agranovich V.M., Ginzburg V.L. *Crystal Optics with Spatial Dispersion, and Excitons* (New York: Springer, 1984; Moscow: Nauka, 1979).
14. Cardona M. *Phys. Status Solidi B,* **220**, 5 (2000).
15. Lastras-Martinez L.F., Ruf T., Konuma M., Cardona M., Aspnes D.E. *Phys. Rev. B*, **61**, 12946 (2000).
16. Ramdas A.K., Rodriguez S., Tsoi S., Haller E.E. *Solid State Commun.*, **133**, 709 (2005).
17. Herrero C.P. *Solid State Commun.*, **110**, 243 (1999).
18. Winer K., Cardona M. *Phys. Rev. B*, **35**, 8189 (1987).